

HNPS Advances in Nuclear Physics

Vol 29 (2023)

HNPS2022



Measurement of differential cross sections for proton elastic scattering on natO at $E_p=4-6$ MeV, suitable for EBS

Michael Kokkoris, Kostas Bosbotinis, Varvara Foteinou, Anastasios Lagoyannis, Fotis Maragkos, Nikolaos Patronis, Evangelia Taimpiri, Anastasia Ziagkova

doi: [10.12681/hnpsanp.5183](https://doi.org/10.12681/hnpsanp.5183)

Copyright © 2023, Michael Kokkoris, Kostas Bosbotinis, Varvara Foteinou, Anastasios Lagoyannis, Fotis Maragkos, Nikolaos Patronis, Evangelia Taimpiri, Anastasia Ziagkova



This work is licensed under a [Creative Commons Attribution-NonCommercial-NoDerivatives 4.0](https://creativecommons.org/licenses/by-nc-nd/4.0/).

To cite this article:

Kokkoris, M., Bosbotinis, K., Foteinou, V., Lagoyannis, A., Maragkos, F., Patronis, N., Taimpiri, E., & Ziagkova, A. (2023). Measurement of differential cross sections for proton elastic scattering on natO at $E_p=4-6$ MeV, suitable for EBS. *HNPS Advances in Nuclear Physics*, 29, 13–19. <https://doi.org/10.12681/hnpsanp.5183>

Measurement of differential cross sections for proton elastic scattering on ^{nat}O at $E_p=4-6$ MeV, suitable for EBS

M. Kokkoris^{1,*}, K. Bosbotinis¹, V. Foteinou², A. Lagoyannis³, F. Maragkos^{1,2}, N. Patronis⁴,
E. Taimpiri^{1,3}, A. Ziagkova^{1,3}

¹ Department of Physics, National Technical University of Athens, Zografou campus, 15780 Athens, Greece

² Central Unit for Ion Beams and Radionuclides, N-Suedstrasse, 44801 Bochum, Germany

³ Tandem Accelerator Laboratory, Institute of Nuclear Physics, N.C.S.R. "Demokritos", Aghia Paraskevi, 15310 Athens, Greece

⁴ Department of Physics, University of Ioannina, 45110 Ioannina, Greece

Abstract In this study we present the experimental differential cross sections of $^{nat}\text{O}(p,p_0)$ elastic scattering, determined via the relative measurement technique, in the proton beam energy range $E_{\text{lab}}=4-6$ MeV with a varying step (from 5-15 keV), at six backscattering detector angles between 120° and 170° (every 10°). A thin, self-supporting target manufactured in the lab was used in this experiment and the determination of its stoichiometry was carried out according to the currently existing evaluation, which has also been benchmarked recently. The measurements were performed using the Van de Graaff Tandem 5.5 MV Accelerator of N.C.S.R. "Demokritos" in Athens, Greece. The differential cross-section datasets obtained in the present work and already existing ones in literature for this extended proton beam energy range are shown and the observed peculiarities and discrepancies are discussed and analyzed.

Keywords Elastic Scattering; EBS; ^{nat}O ; Differential cross sections

INTRODUCTION

Oxygen is Earth's most abundant element, and after hydrogen and helium, it is the third-most abundant element in the universe. Naturally occurring oxygen is composed of three stable isotopes, ^{16}O , ^{17}O , and ^{18}O , with ^{16}O being the most abundant (99.762% in ^{nat}O). Diatomic oxygen gas currently constitutes 20.95% of the Earth's atmosphere and makes up almost half of the Earth's crust in the form of oxides. It is a highly reactive non-metal and thus, it can easily form compounds with other elements and penetrate or diffuse deeply inside several matrices. Therefore, the accurate determination of oxygen depth profiles in various samples is of paramount importance, especially in the semiconductor industry, or, e.g., in biological, geological, cultural heritage materials and superconductors. For this purpose, Ion Beam Analysis (IBA) techniques have proven to be very effective, and more specifically, the proton elastic backscattering spectroscopy (p-EBS) one, which is currently widely used for the detection of almost all the light elements up to a depth of several microns, while d-NRA and ToF-ERDA are usually employed at smaller depths. For the implementation of EBS, evaluated differential cross sections are required, which are the most reliable ones and are usually the result of R-matrix calculations based on several experimental differential cross-section datasets. These evaluated datasets are provided by the online R-matrix SigmaCalc 2.0 calculator (<http://sigmacalc.iate.obninsk.ru/>). In the particular case of oxygen, the current evaluated data for protons cover the energy range between 100 and 4080 keV, based on the pioneer work of A.F. Gurbich [1]. However, the goal to investigate oxygen concentrations at even greater depths, according to the current technological demands, is currently impeded by the relative lack of experimental and, consequently, evaluated data at higher proton beam energies. Only three relevant differential cross-section datasets exist [2-4] and none of them is focused on the implementation of IBA techniques. The existence of several coherent datasets for elastic scattering over a broad angular and energy range is important, as it permits the detailed theoretical investigation of the

* Corresponding author: kokkoris@central.ntua.gr

obtained differential cross sections and the accurate tuning of the relevant nuclear parameters.

In order to address this problem, in the present work we determined the experimental differential cross sections of $^{nat}\text{O}(p,p_0)$ elastic scattering via the relative measurement technique, in the proton beam energy range $E_{\text{lab}}=4\text{--}6$ MeV with a varying step (from 5-15 keV), at six backscattering detector angles, ranging between 120° and 170° (with a 10° step). A thin, solid, self-supporting target, rich in oxygen and manufactured in the lab was used in this experiment and the determination of its stoichiometry was carried out according to the currently existing evaluation obtained via SigmaCalc 2.0, which has also been benchmarked recently [5]. The measurements were performed using the Van de Graaff Tandem 5.5 MV Accelerator of N.C.S.R. “Demokritos” in Athens, Greece.

EXPERIMENTAL DETAILS

The whole experimental procedure included two distinct phases, namely the study of the thin target thickness and the determination of the differential cross-section values. Both phases were carried out using the proton beam of the 5.5 MV TN11 HV Tandem Accelerator of N.C.S.R. “Demokritos”, Athens, Greece. For the cross-section measurements, protons, accelerated to $E_{p,\text{lab}}=4000\text{--}6000$ keV, were directed to a large-size, cylindrical scattering chamber (radius: 40 cm) equipped with a high-precision goniometer (0.1°). The final energy of the proton beam was determined by Nuclear Magnetic Resonance (NMR) with an estimated ripple of ~ 1.6 keV (considered stable for the whole energy interval studied) as verified at the beginning of the experiment – using protons – by the reaction rate of the 991.89 keV resonance ($\Gamma=110$ eV) of the $^{27}\text{Al}(p,\gamma)$ reaction, using a 18% relative efficiency HPGe detector, placed close to a thick aluminum foil mounted inside the Faraday cup. The corrected energy values were subsequently used for the ADC energy calibration, whose linearity was proven to be excellent (better than 0.4%). The differential cross sections were obtained using a variable beam energy step of 5-15 keV, tuned according to the expected structure of the measured excitation functions.

The target was placed at a distance of $\sim 9\text{--}12$ cm from the detectors and orthogonal slits ($\sim 3.5 \times 9$ mm²) were mounted in front of them to reduce the azimuthal angular uncertainty ($< \pm 1^\circ$), while allowing for an adequate effective solid angle to be subtended by the detectors. Additionally, small cylindrical aluminum tubes, with variable lengths ($\sim 3\text{--}5$ cm) and having a diameter of ~ 1.1 cm, were placed in front of the detectors to eliminate any possible excessive background under the oxygen elastic peak due to scattering in the chamber walls and/or in the Faraday cup. The presence of the tubes did not affect the subtended solid angle, nor introduced any other additional background, as verified experimentally.

The detection system consisted of six Si surface barrier detectors, having a thickness of 500 μm , set at 10° intervals, between 120° and 170° , along with the standard corresponding nuclear spectroscopy electronics. The beam spot size was limited to $\sim 2 \times 2$ mm², while the current on the target did not exceed ~ 200 nA during all the measurements, aiming to avoid any significant pileup effects and/or the overheating of the thin target. The experimental spectra from all the detectors were simultaneously recorded via centrally controlled independent ADCs and the procedure was repeated at every $E_{p,\text{lab}}$. The vacuum was kept constant during all the measurements, being as low as $\sim 5 \times 10^{-7}$ Torr. A typical spectrum is shown in Fig. 1a for $E_{p,\text{lab}} \sim 5050$ keV taken at 120° in logarithmic scale for reasons of clarity, along with the corresponding peak identification.

The latest version of SIMNRA (v.7.03) [6] was used in order to calculate the mean proton beam energy at half the target’s thickness, following the determination of the target composition via the analysis of proton spectra taken at $E_{p,\text{lab}}=2000, 2300, 3200$ and 3900 keV (the specific energies were selected in order to avoid any strong, steep resonances) exactly for this purpose, using the same experimental setup, while the simulations involved only the detectors set at steep backward angles, namely at $140^\circ, 150^\circ, 160^\circ$ and 170° . For the analysis of the EBS spectra a very small energy step was set for the incoming and outgoing protons, and the exact detector geometry, the effect of multiple

scattering, the beam ripple, the latest SRIM2013 [7] stopping power data, and Chu and Yang's straggling model were considered, as implemented in the SIMNRA code.

The target used for the differential cross-section measurements was a thin, self-supported, multi-layered structure, created *in situ*, using the evaporation technique, as follows: The substrate consisted of a thin carbon accelerator stripping foil, on top of which a layer of disodium phosphate (Na_2HPO_4) was evaporated and, on top of this, an ultra thin Au layer was also subsequently evaporated for normalization and wear protection purposes. The lateral homogeneity of the target structure was experimentally tested by slightly changing its position (yielding differences less than 5%), while its thermal and mechanical stability proved to be excellent throughout the whole period of measurements.

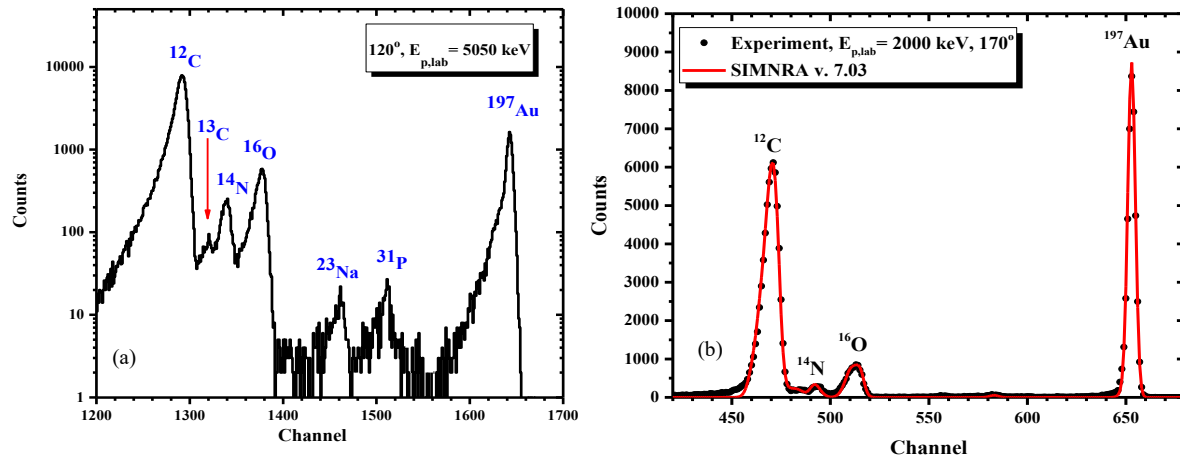


Figure 1. (a) A typical experimental spectrum taken at $E_{p,\text{lab}} \sim 5050 \text{ keV}$ and at 120° , demonstrating the good separation of the oxygen peak under study. The spectrum is shown in logarithmic scale and all the existing peaks are identified. (b) Experimental and simulated spectrum of the thin target taken at $E_{p,\text{lab}} \sim 2000 \text{ keV}$, 170° .

RESULTS AND DISCUSSION

As mentioned in the previous paragraphs, the differential cross sections were determined using the corresponding formula of the relative measurement technique [8]:

$$\left(\frac{d\sigma}{d\Omega}\right)_{E,\theta}^N = \left(\frac{d\sigma}{d\Omega}\right)_{E',\theta}^{\text{Au,Ruth}} \times \frac{Y_{\text{O}}}{Y_{\text{Au}}} \times \frac{N_{\text{Au}}}{N_{\text{O}}},$$

where θ corresponds to the scattering angle seen by each detector, E and E' represent the energies at the half of the target's thickness and at the surface of the target (following the accelerator energy calibration), respectively, Y_{O} and Y_{Au} are the integrated yields as obtained from the experimental spectra and $N_{\text{Au}}/N_{\text{O}}$ is the ratio of the total number of Au versus ^{16}O nuclei existing in the target.

The differential cross-sections of proton elastic scattering from gold, $\left(\frac{d\sigma}{d\Omega}\right)_{E',\theta}^{\text{Au,Ruth}}$, were calculated according to the Rutherford formula (along with the appropriate screening corrections) over the whole energy range under study ($E_{p,\text{lab}} = 4000\text{--}6000 \text{ keV}$).

Tv [9], a standard, freely-distributed linux-based code for nuclear spectroscopy, developed at the University of Karlsruhe (Germany) was used for peak fitting/integration and background subtraction. As shown in Fig. 1(a), there was no significant peak overlap, or induced background contribution under the oxygen and gold elastic peaks over the whole energy range under study. Moreover, the small nitrogen parasitic contribution was clearly separated from the oxygen peak. The statistical error in Y_{Au} was always kept below 2%, while the corresponding one in Y_{O} did not exceed 2-3% in the least favorable case.

The accurate determination of the $N_{\text{Au}}/N_{\text{natO}}$ ratio is probably the most critical factor for the determination of the differential cross-section values using the relative technique. Since proton elastic

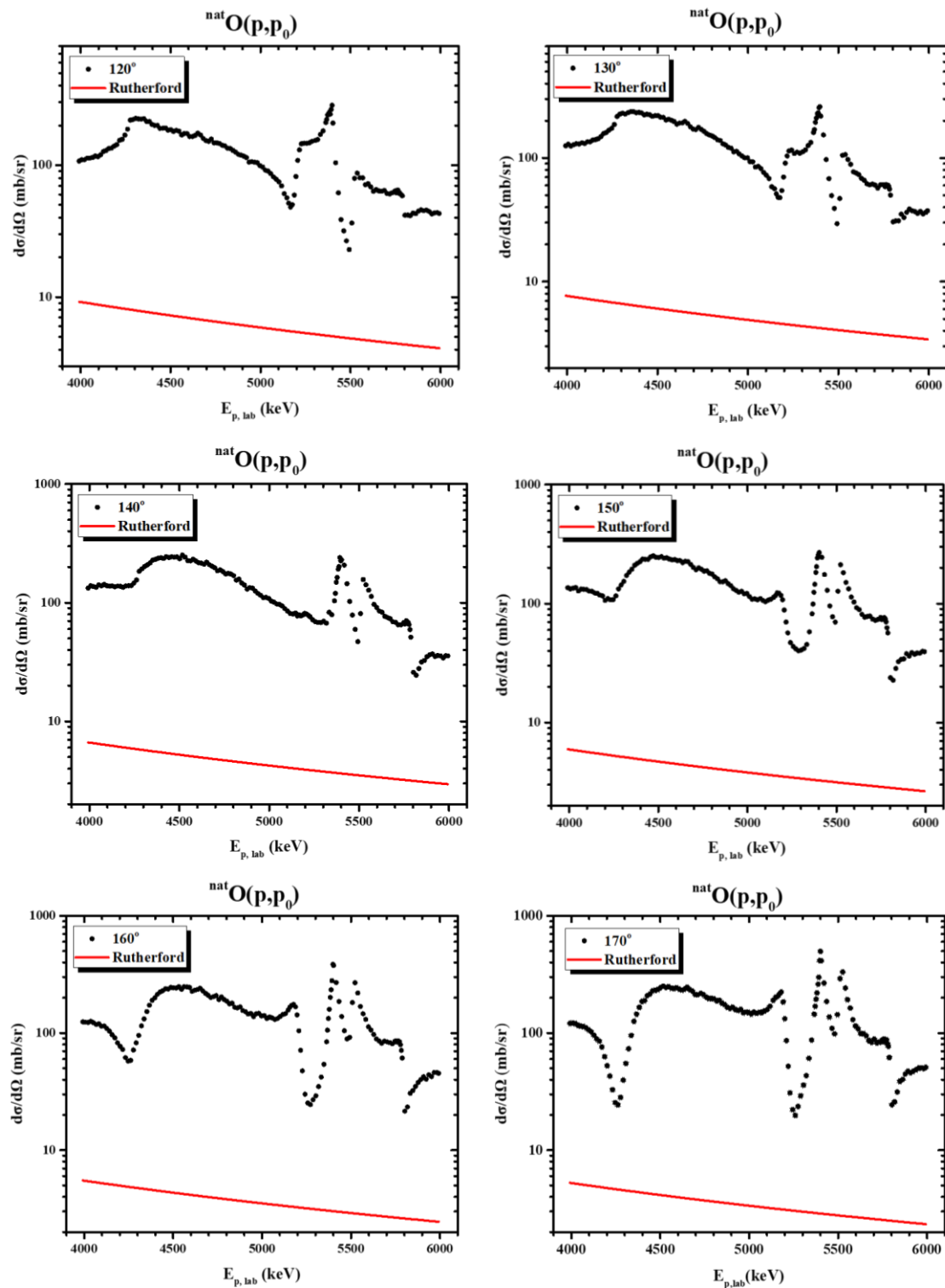


Figure 2a-f. Differential cross-section values (mb/sr) of the $^{nat}O(p,p_0)$ elastic scattering, determined at $E_{p,lab}$ 4000–6000 keV and for the scattering angles of 120°, 130°, 140°, 150°, 160° and 170°, along with the corresponding values obtained using the Rutherford formula. The total estimated uncertainties (excluding the systematic errors) are included in the graphs; in the x-axis, the errors are not visible due to the adopted scale.

scattering on oxygen has been well evaluated and benchmarked [1, 5], dedicated proton elastic backscattering spectra were taken within the energy range covered by the current evaluation and were subsequently analyzed using SIMNRA as follows: The $Q \times \Omega$ product was set arbitrarily as to accurately

reproduce the Au peak, and then the ^{nat}O content in the target was varied aiming at reproducing the total amount of integrated oxygen counts, using the non-Rutherford evaluated data for proton elastic scattering on ^{nat}O , obtained from SigmaCalc 2.0. Following this procedure, the total Au and O thickness (in atoms/cm²) was determined for every proton beam/scattering angle combination under study, by slightly varying the target composition in each case. The average value of the $N_{\text{Au}}/N_{\text{natO}}$ ratio was thus determined to be 0.275 ± 0.005 , with a relative statistical error of $\sim 1.8\%$. This error does not include any systematic uncertainties, originating mainly from the accuracy of the implemented stopping power compilation, lateral inhomogeneities in the target composition and carbon buildup effects, which –in any case– did not exceed 7% (in total). Especially in the case of protons impinging on oxygen, reported deviations between compiled and experimental stopping-power data can be as low as 2.3% [7]. An example of the target simulation is shown in Fig. 1(b) for the proton beam energy of 2000 keV, taken at 170°, along with the corresponding peak identification, revealing the excellent reproduction of the experimental proton EBS spectrum, obtained without any change in the positioning of the target.

Following this simulation, the average obtained target composition was used for the determination of E , at each beam energy step, as follows: $E = E' - \Delta E_{\text{Au}} - \Delta E_{\text{O}/2}$, where E' corresponds to the corrected accelerator energy, ΔE_{Au} corresponds to the energy loss in the ultra thin surface gold layer and $\Delta E_{\text{O}/2}$ to the energy loss considering half of the disodium phosphate target thickness. These E values were subsequently used as the appropriate reference x-values in the corresponding differential cross-section figures.

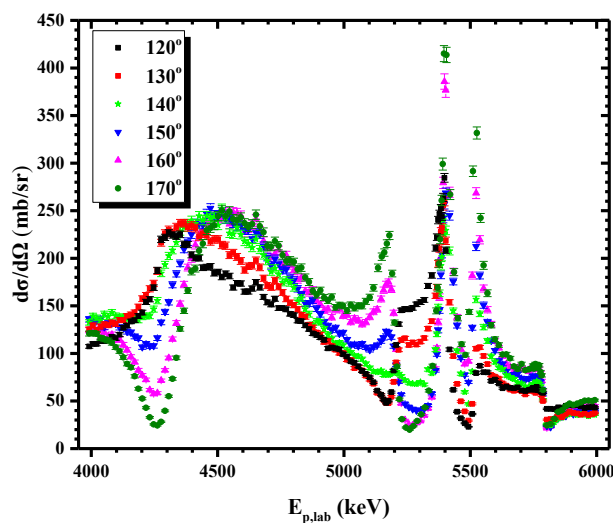


Figure 3. Demonstration of the strong energy and angular variation of the obtained differential cross-section datasets

The differential cross-section values obtained in the present work for the proton elastic scattering on oxygen, $^{nat}\text{O}(p,p_0)$, for the six studied backscattering angles (120°, 130°, 140°, 150°, 160°, 170°) are presented in Figs.2a–f, along with the values obtained using the Rutherford formula. The combined experimental statistical uncertainty did not exceed $\sim 5\%$ in all cases, while the error in energy was ~ 6 keV (including the accelerator energy ripple and the beam straggling inside the target). It should be noted here that the $\sigma_{\theta}(\text{elastic})/\sigma_{\theta}(\text{Rutherford})$ ratio varies between ~ 5 and over ~ 150 , implying that the EBS analysis of oxygen using high-energy protons can be proven to be highly advantageous, even in the case of low oxygen concentrations present in heavy matrices. It should be noted here, however, that, as shown in Fig.3, where all the determined differential cross sections are plotted together, there exists a quite strong angular and energy variation, therefore, particular care should be given by the users to

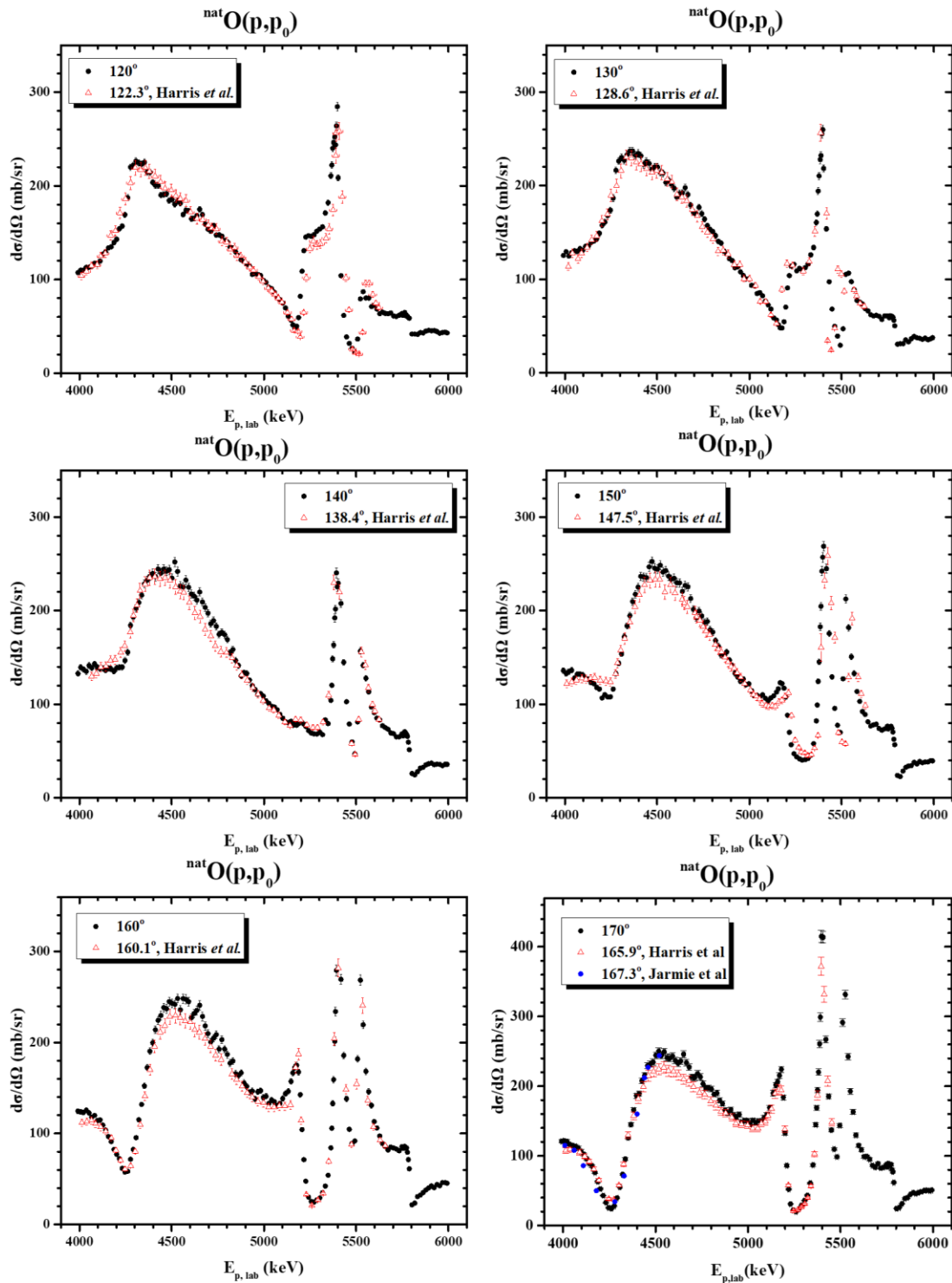


Figure 4a–f. Differential cross-section values (mb/sr) of the $^{nat}O(p,p_0)$ elastic scattering, measured at $E_{p,lab}$ 4000–6000 keV and for the scattering angles of 120° , 130° , 140° , 150° , 160° and 170° , along with data from literature [2-3]. The total estimated uncertainties (excluding the systematic errors) are included in the graphs for all cases; in the x-axis, the errors are practically not visible due to the selected scale.

the accurate positioning of the SSB detector used for oxygen depth profiling, while the accelerator proton beam energy should also be known with high precision. All the results will soon be available to the scientific community at the IBANDL website (<https://www-nds.iaea.org/exfor/ibandl.htm>), in both tabulated and graphical forms.

The values obtained in the present work are also plotted in Figs. 4a-f, along with results from previous measurements, according to the closest experimental angle under study [2, 3]. The only results that have been omitted are those from S. R. Salisbury *et al* [4], because the official digitization of the graphs by the EXFOR library has not been performed yet. As shown in Figs. 4a-f, the results from the present work are generally in very good agreement with those obtained in the past. With the notable exception of relatively low proton beam energies, namely below 4300 keV, most of the determined values are even within the quoted errors with those obtained in the past by Harris *et al.* [2] and Jarmie *et al.* [3], although the overlap of the latter with the present datasets is really limited, whilst the overlap with those determined in [2] is much more extended. The agreement with the results from [4] is also excellent, with the exception of one angle, where there is a clear shift in the energy of the resonances. It should also be mentioned that, as far as [2] is concerned, there is also a strange energy shift of ~22 keV and ~50 keV at 120° and 130° respectively, which seriously affects the high-energy resonances. The corresponding shift is ~45 keV for the detection angle of 150°, while it is minimal, or even non-existent for the other scattering angles (140°, 160° and 170°). There is no clear explanation for this discrepancy, despite the *ab initio* different method for the accelerator energy calibration adopted in [2]. Still, despite the energy shifts, the quite impressive overall agreement between the datasets obtained in the present work and those reported by Harris *et al.*, can constitute a firm, encouraging base for the subsequent theoretical investigation of proton elastic scattering on ^{nat}O at high beam energies.

CONCLUSIONS

In the present work the elastic backscattering of protons from ^{nat}O has been studied between 120° and 170° and coherent experimental differential cross-section datasets have been determined, suitable for EBS applications. These datasets can facilitate the accurate quantitative determination of oxygen depth profile concentrations inside several complex matrices.

While it is undoubtedly true that there is a certain lack of experimental differential cross-section datasets suitable for large-depth EBS applications, especially in the case of oxygen, this theoretical analysis can prepare the ground for a future extension of the SigmaCalc 2.0 evaluation at higher energies. It is the authors' firm belief that the present work concerning oxygen, along with the ongoing efforts to extend the SigmaCalc 2.0 evaluation for nitrogen to higher proton beam energies, complement the successful corresponding work on carbon [10] and, when completed, they will significantly enhance the p-EBS capabilities, at least for the main light elements of high technological interest.

Acknowledgments

The authors gratefully acknowledge the financial support by the PEVE-2020 program of NTUA

References

- [1] A.F. Gurbich, Nucl. Instr. and Meth. in Phys. Res. B129, 311 (1997)
- [2] R.W. Harris, G.C. Phillips, C. Miller-Jones, Nuclear Physics 38, 259 (1962)
- [3] N. Jarmie and J.D. Seagrove, Los Alamos Report LA-2014 (1957)
- [4] S.R. Salisbury *et al.*, Phys. Rev. 126 (6), 2143 (1962)
- [5] M. Kokkoris *et al.*, Nucl. Instr. and Meth. in Phys. Res. B405, 50 (2017)
- [6] M. Mayer, Nucl. Instr. and Meth. in Phys. Res. B332, 176 (2014)0
- [7] J.F. Ziegler, M.D. Ziegler, J.P. Biersack, Nucl. Instr. and Meth. in Phys. Res. B268, 1818 (2010)
- [8] E. Ntemou, A.F. Gurbich, M. Kokkoris, A. Lagoyannis, Nucl. Instr. and Meth. in Phys. Res. B510, 56 (2022)
- [9] J. Theuerkauf, S. Esser, S. Krink, M. Luig, N. Nicolay, O. Stuch, H. Wolters, Program tv, Institute for Nuclear Physics, Cologne (2007)
- [10] D. Abriola, A.F. Gurbich, M. Kokkoris, A. Lagoyannis, V. Paneta, Nucl. Instr. and Meth. in Phys. Res. B269, 2011 (2011)